

## Production and dispersion stability of nanoparticles in nanofluids

Yujin Hwang<sup>a</sup>, Jae-Keun Lee<sup>a</sup>, Jong-Ku Lee<sup>c</sup>, Young-Man Jeong<sup>a</sup>, Seong-ir Cheong<sup>a</sup>,  
Young-Chull Ahn<sup>b</sup>, Soo H. Kim<sup>d,\*</sup>

<sup>a</sup> Department of Mechanical Engineering, Pusan National University, San 30, Jangjeon-dong, Geumjeong-gu, Busan, 609-735, South Korea

<sup>b</sup> School of Architecture, Pusan National University, San 30, Jangjeon-dong, Geumjeong-gu, Busan, 609-735, South Korea

<sup>c</sup> LG Electronics, Gaeumjeong-dong, Changwon City, Gyeongnam, 641-711, South Korea

<sup>d</sup> Department of Nanosystem and Nanoprocess Engineering, Pusan National University, San 30, Jangjeon-dong, Geumjeong-gu, Busan, 609-735, South Korea

Received 11 October 2006; received in revised form 8 November 2007; accepted 12 November 2007

Available online 23 November 2007

### Abstract

This paper presents an experimental study on the homogeneous dispersion of nanoparticles in nanofluids. In this study, various physical treatment techniques based on two-step method, including stirrer, ultrasonic bath, ultrasonic disruptor, and high-pressure homogenizer were systematically tested to verify their versatility for preparing stable nanofluids. Initially carbon black and silver nanoparticles dispersed in base fluids with the presence of surfactant were found to be highly agglomerated with the hydrodynamic diameter of 330 nm to 585 nm, respectively. After both CB and Ag nanofluids were treated by various two-step methods, stirrer, ultrasonic bath, and ultrasonic disruptor was found to do a poor performance in deagglomeration process for the initial particle clusters. However, the high-pressure homogenizer produced the average diameter of the CB and Ag particles of 45 nm and 35 nm, respectively, indicating that among various physical treatment techniques employed in this study, the high-pressure homogenizer was the most effective method to break down the agglomerated nanoparticles suspended in base fluids. In order to prepare another nanofluid with much smaller primary nanoparticles, we also employed a modified magnetron sputtering system, in which the sputtered nanoparticles were designed to directly mix with the running surfactant-added silicon oil thin film formed on a rolling drum (i.e. one-step method). We observed that Ag nanoparticles produced by the modified magnetron sputtering system were homogeneously dispersed and long-term stable in the silicon oil-based fluid, and the average diameter of Ag nanoparticles was found to be  $\sim 3$  nm, indicating that the modified magnetron sputtering system is also an effective one-step method to prepare stable nanofluids.

© 2007 Elsevier B.V. All rights reserved.

**Keywords:** Nanofluids; Magnetron sputtering; Stability; Zeta potential; High-pressure; Homogenizer; Nanoparticle

### 1. Introduction

It has long been recognized that the suspensions of solid particles in liquids provide useful advantages in industrial fluid systems, including heat transfer fluid, magnetic fluid, and lubricant fluid [1–5]. Since the working fluids have the limitation of heat transfer performance, solid particles were

dispersed in the working fluids to improve their thermal properties or heat transfer characteristics [2,6–9]. However, those previous practical applications were mostly confined to the suspensions with millimeter or micrometer-sized particles, which tended to quickly settle down and subsequently resulted in severe clogging in micro-channels.

Unlike micrometer-sized particle suspensions, nanoparticle-based fluids (i.e. nanofluids) were recently reported to be much more stable due to vigorous Brownian motion of suspended nanoparticles in the base fluids [10,11]. Even though various methods have been developed to prepare nanofluids, those previous approaches still had instability problems caused by

\* Corresponding author. Tel.: +82 55 350 5287; fax: +82 51 512 5236.

E-mail address: [sookim@pusan.ac.kr](mailto:sookim@pusan.ac.kr) (S.H. Kim).

Table 1  
Test conditions and materials for producing nanofluids

	Nanofluids	
	CB–water	Ag–silicon oil
Particles	CB (carbon black) Primary size: 40 nm Weight percentage: 0.5 wt%	Ag (silver) Primary size: 35 nm Weight percentage: 0.5 wt%
Basefluid	DI-water Viscosity: 0.87 mm <sup>2</sup> /s	Silicon oil (DC-704) Viscosity: 39 mm <sup>2</sup> /s
Surfactant	SDS (Sodium dodecyl sulfate) Weight percentage: 1 wt%	Oleic acid Weight percentage: 1 wt%

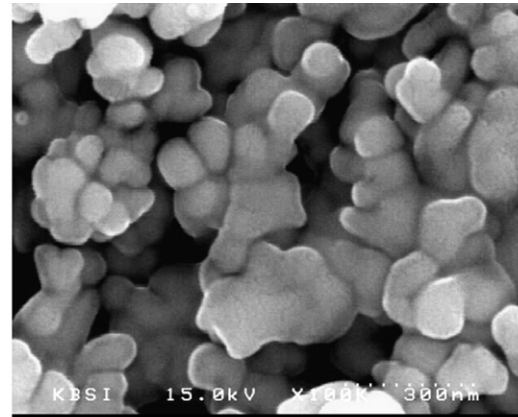
particle agglomeration in the base fluids. In order to prepare stable nanofluids, numerous investigations on colloidal dispersions have been conducted in view of particle motion analysis in various flow conditions and sedimentation characteristics studies on suspended nanoparticles in base fluids [12–14]. Among the various nanofluid preparation methods, the addition of surfactants was known to be effective to homogeneously disperse nanoparticles in the base fluids [15,16]. The surfactants (e.g. sodium dodecyl sulfate (SDS)) resulted in the electrostatic repulsion between surfactant-coated nanoparticles, which significantly reduces the particle agglomeration due to van der Waals forces of attraction [17].

There are two major methods for producing nanofluids; (i) the one-step direct evaporation method represents the direct formation of the nanoparticles inside the base fluids, and (ii) the two-step method represents the formation of nanoparticles and subsequent dispersion of the nanoparticles in the base fluids. In either case, the preparation of a uniformly dispersed nanofluid is essential for obtaining stable reproduction of physical properties or superior characteristics of the nanofluids [4,18]. Although many experimental studies on nanofluid systems have been performed, the preparation methods for stable nanofluids were not systematically studied yet. In this work, we employed various physical treatment techniques, including a stirrer, an ultrasonic bath, an ultrasonic disruptor, a high-pressure homogenizer, and a modified magnetron sputtering system to prepare nanofluids, and then we observed the effect of each nanofluid preparation technique on the suspended nanoparticle size, morphology, and dispersity in the water- or silicon oil-based fluids.

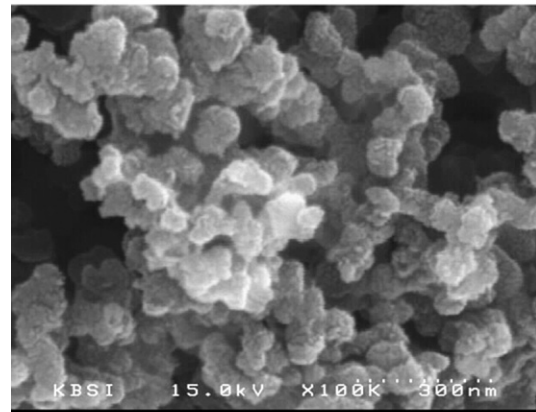
## 2. Materials and methods

### 2.1. Materials

Table 1 shows the specification of two materials used for producing nanofluids. First, carbon black (CB) nanoparticles were dispersed in deionized (DI) water with initial concentration of 0.5 wt%. The primary size of CB nanoparticle was 40 nm. Second, Ag nanoparticles were mixed with silicon oil (DC-704, Dow Corning Inc.) with the initial concentration of 0.5 wt.%, and the primary size of Ag nanoparticles was 35 nm. To prevent the agglomeration between primary nanoparticles in the base fluid, either SDS or oleic acid was added as the surfactants to coat the surface of CB and Ag nanoparticles,



(a) Ag nanoparticles



(b) CB nanoparticles

Fig. 1. SEM images of the tested nanoparticles.

respectively. The surfactants were added in each base fluid with the concentration of 1 wt.%. Fig. 1 shows the scanning electron microscope (SEM) images of Ag and CB nanoparticles before dispersing them into the base fluid. Both SEM images show that the particles were highly agglomerated.

### 2.2. Methods

Table 2 summarizes the detailed experimental conditions of various nanofluid preparatory methods employed in this study.

Table 2  
The methods of producing nanofluids

Method of producing nanofluid		Test condition
Two-step method	Stirrer	Revolution speed: 1500 rpm Revolution time: 120 min
	Ultrasonic bath	Sonication time: 60 min Frequency: 40 kHz
	Ultrasonic disruptor	Sonication time: 60 min Frequency: 20 kHz Max. sonicating power: 350 W
	High-pressure homogenizer	Number of pass: 3 Pressure: 18,000 psi
One-step method	Magnetron sputtering	DC power: 0.2 kV Ar gas mass flow rate: 25 cm <sup>3</sup> /min

In the two-step method, nanoparticles were first separately produced, and then the prepared nanoparticles were dispersed in the base fluid with the assistance of various physical treatment techniques, including the stirrer, the ultrasonic bath, the ultrasonic disruptor, and the high-pressure homogenizer, which will be described in detail later. These two-step methods were aimed at deagglomerating the particle clusters in order to obtain homogeneous suspensions. In the one-step method, we employed the modified magnetron sputtering technique, in which Ag nanoparticles were formed by direct condensation of Ag vapor produced by the magnetron sputtering, and subsequently the Ag nanoparticles hit the surface of low vapor pressure liquid film formed by a rotating drum, which soaked in the surfactant-presented base liquid. In this one-step method, we aimed at developing a method to prepare a stable nanofluid with isolated smaller primary particles by shortening the particle travel distance so that the coagulation process between the primary particles formed in the gas phase was significantly reduced.

In this study, CB–water and Ag–silicon oil nanofluids were produced by the two-step methods. Also another Ag–silicon oil nanofluid was produced by the one-step method for comparison purpose. The size distribution and zeta potential of nanoparticles suspended in nanofluids were measured by an electro-phoretic light scattering (ELS) particle counter (Model No. ELS-8000, Otsuka Electronics Inc.), which consisted of a laser source, a scattering cell, electrodes for applying an electric field, a photomultiplier, and a spectrum analyzer. Operating principle of the ELS is described in detail elsewhere [19,20]. Briefly, the charged particles in the scattering cell were forced to move along the applied electric field. This particle motion resulted in

Doppler shift of scattered laser light detected by the spectrometer. The detector signal was then sent to a digital correlator, and subsequently the resulting autocorrelation function was analyzed to find the information of the distribution of particle velocities and diffusion constant of moving particles. Then the diffusion constant was used to determine the Stokes diameter of suspended particles [21]. Here Stokes diameter is defined by the diameter of spherical particle with same velocity and density of the suspended particle. And the zeta potential was extracted from the relation of particle mobility, fluid viscosity, and dielectric constant of liquid [22]. The measured size with this method is that of primary particles or clusters of particles in motion. This real size distribution of the particles of clusters is so called “hydrodynamic diameter” in the suspension.

The stirrer used in preparing CB–water and Ag–silicon oil nanofluids had 4 blades. The revolution speed and time of blades were 1500 rpm and 2 h, respectively. Two types of sonicators were also employed in this study. One was the ultrasonic bath (40 kHz) and the other was the ultrasonic disruptor (20 kHz, 350 W). Ultrasonic wave has been transferred to the test sample through water for the ultrasonic bath while it has been propagated directly to the test sample from a vibrating horn for the ultrasonic disruptor. The suspensions were sonicated for 1 h for both the ultrasonic bath and disruptor. There was no appreciable change in suspended particle morphology with more than 1 hour sonication.

As another two-step method for producing a nanofluid, we employed a high-pressure homogenizer (Model No. M-110LCE, Microfluidics, Inc.). Fig. 2 presents the schematic diagram of the high-pressure homogenizer, which is consisted of two micro-channels, dividing a liquid stream into two streams.

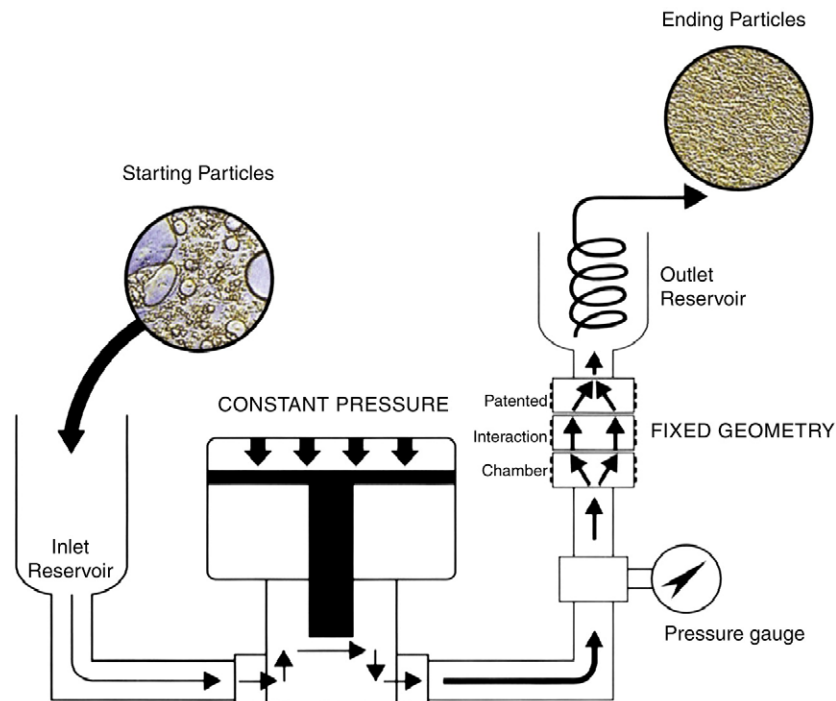


Fig. 2. Schematic diagram of the high-pressure homogenizer for producing nanofluids.

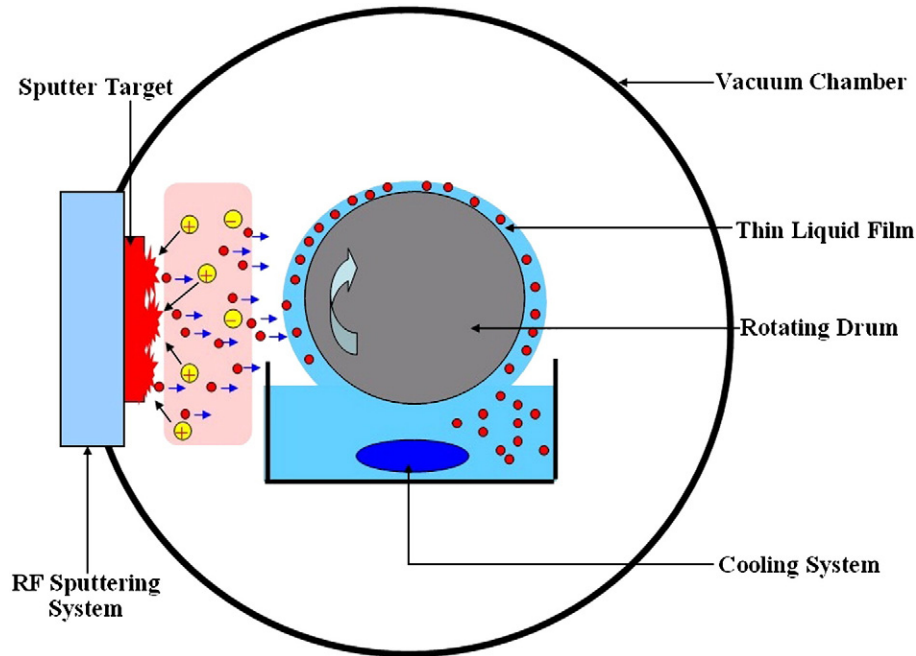


Fig. 3. Schematic diagram of the modified magnetron sputtering system for producing nanofluids.

The both liquid streams divided were then recombined in a reacting chamber. Here the significant increase in the velocity of pressurized liquid streams in the micro-channels resulted in the formation of cavitations in the liquid [23]. The high energy of cavitations was used to break the clusters of nanoparticles [24]. In this work, the nanoparticle suspension flows through a tube with the inner diameter of 3 mm prior to the interaction chamber in the high-pressure homogenizer. When the suspension reached inside the interaction chamber, it is designed to flow through the microchannel with the inner diameter of 75  $\mu\text{m}$ . In such a contracting flow condition, the flow velocity of the suspension flowing through the microchannel should be increased up to  $\sim 1600$  times according to Bernoulli's theorem, and simultaneously cavitation phenomena are significantly occurred. In this fast flow region, particle clusters must be broken by the combination of various mechanisms, including (i) strong and irregular impactation on the wall inside the interaction chamber, (ii) microbubbles formed by cavitation-induced exploding energy, and (iii) high shear rate of flow. This leads us to finally obtain very homogeneous suspensions with less aggregated particles. CB–water and Ag–silicon oil nanofluids were produced at the applied pressure of 18,000 psi, and then the nanofluids were passed through the high-pressure homogenizer over 3 times repeatedly to obtain sufficiently homogeneous nanoparticle distribution in the base fluids. As the results shown later, the particle clusters has been broken into the size of the primary particle size after 3 pass treatment at the pressure of 18,000 psi.

As a one-step method, we also employed the modified magnetron sputtering system. Fig. 3 shows the schematic diagram of the magnetron sputtering system for producing nanofluids [25,26]. The vacuum in the chamber was pumped

down to  $1 \times 10^{-6}$  torr by a diffusion pump. After filling the chamber with argon (Ar) gas up to a desired gas pressure, a constant Ar gas flow rate ranging from 15 to 50  $\text{cm}^3/\text{min}$  was adjusted. The sputtering Ar gas pressure was fixed at  $1 \times 10^{-2}$  torr for producing Ag nanoparticles. The target substrate was a rotating drum dipped into the reservoir of silicon oil. The rotational speed was varied from 0 to 10 rpm. The distance between Ag sputtering target and drum was fixed to 8 cm. The Ag particles sputtered directly dispersed in the thin film of silicon oil formed on the rotating drum. To avoid agglomeration of the Ag particles, the oleic acid (1 wt.%) was dissolved in the base fluid prior to the sputtering process. For a transmission electron microscope (TEM) sample preparation, TEM grid was manually dipped into the sonicated solution, which had the mixing ratio of particle suspension:acetone = 1:10 in volume.

### 3. Results and discussion

To see the effect of physical treatment on the suspended particle morphology, we performed TEM analysis for two-step method-assisted CB nanoparticles in DI-water nanofluids seen in Fig. 4. Without any physical treatment, CB nanoparticles with surfactant were highly agglomerated in DI-water (see Fig. 4a). After using the stirrer, there was no appreciable change in particle morphology (see Fig. 4b) However, after using the ultrasonic bath and ultrasonic disrupter, the size of agglomerated particles and number of primary particles in a particle cluster was significantly decreased (see Fig. 4c and d). As one can see in Fig. 4e, the high-pressure homogenizer was found to be the most effective method to deagglomerate the CB nanoparticles in the suspensions.



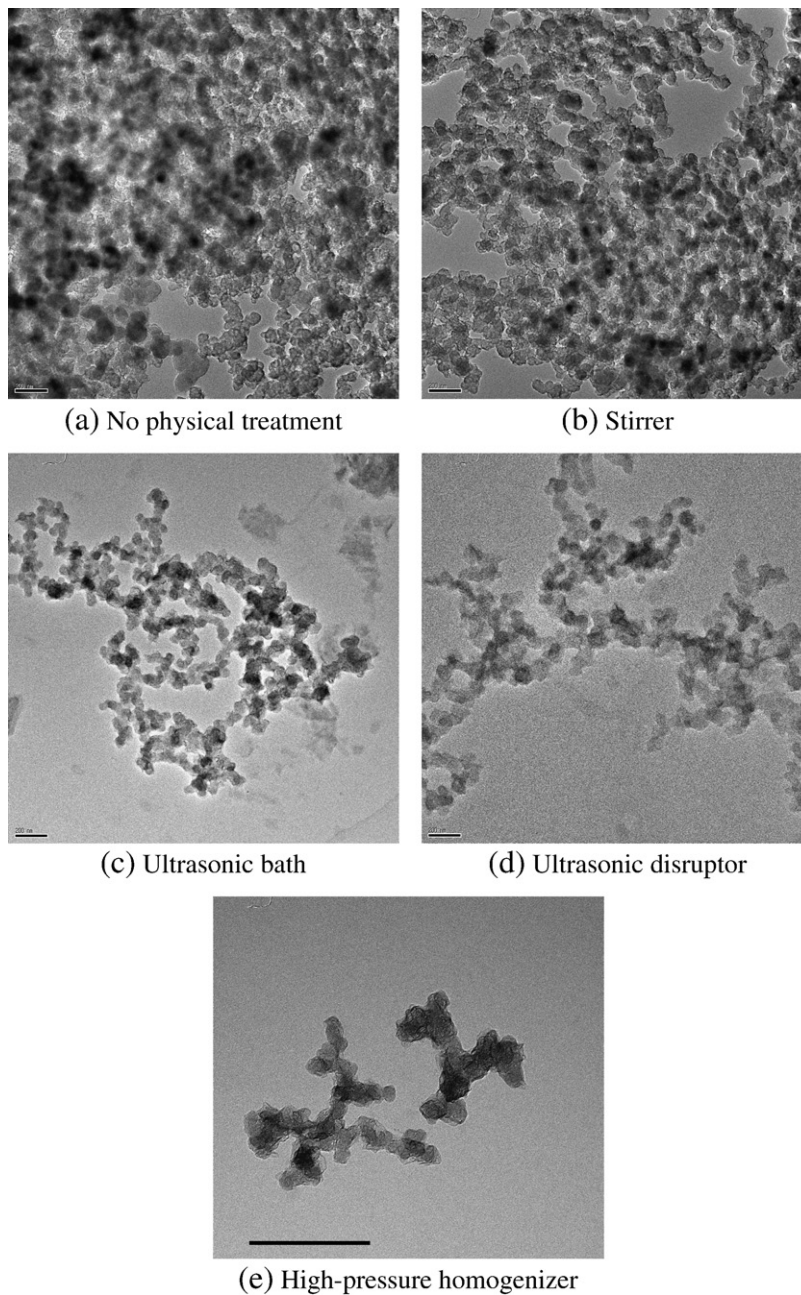


Fig. 4. TEM images of CB nanoparticles in water-based nanofluids prepared by two-step methods. (The inserted scale bar is 200 nm).

Fig. 5 shows TEM images of Ag nanoparticles in silicon oil-based nanofluids. Without any physical treatment, the Ag nanoparticles dispersed in silicon oil with the presence of surfactants were observed to have high level of agglomeration in the silicon oil, and the average diameter of Ag particles was found to be 335 nm. As previously observed from CB–water nanofluids, the stirrer does not seem to be an effective method to break down the size of the Ag nanoparticle clusters (see Fig. 5b). Even both sonication methods did not seem to provide sufficient energy to break the particle clusters as seen in Fig. 5c and d. The high-pressure homogenizer was found to effectively break down the agglomerated particles as seen in Fig. 5e. The particle morphology in Fig. 5e is a little bit

different with the others. When a suspension go through the microchannel inside the interaction chamber, particle clusters in the suspension undergo extremely strong impactions on the inside wall of the interaction chamber, which is coated with a diamond layer in this study. Because diamond coating layer has much higher hardness than silver, silver nanoparticles was presumably worn and rounded by the strong impaction, which resulted in a little different morphologies.

To corroborate the effect of each physical treatment on the level of particle deagglomeration, we measured particle size distributions for each CB–DI-water and Ag–silicon oil nanofluid prepared by two-step methods as shown in Fig. 6. Without any physical treatments, the average diameter of CB

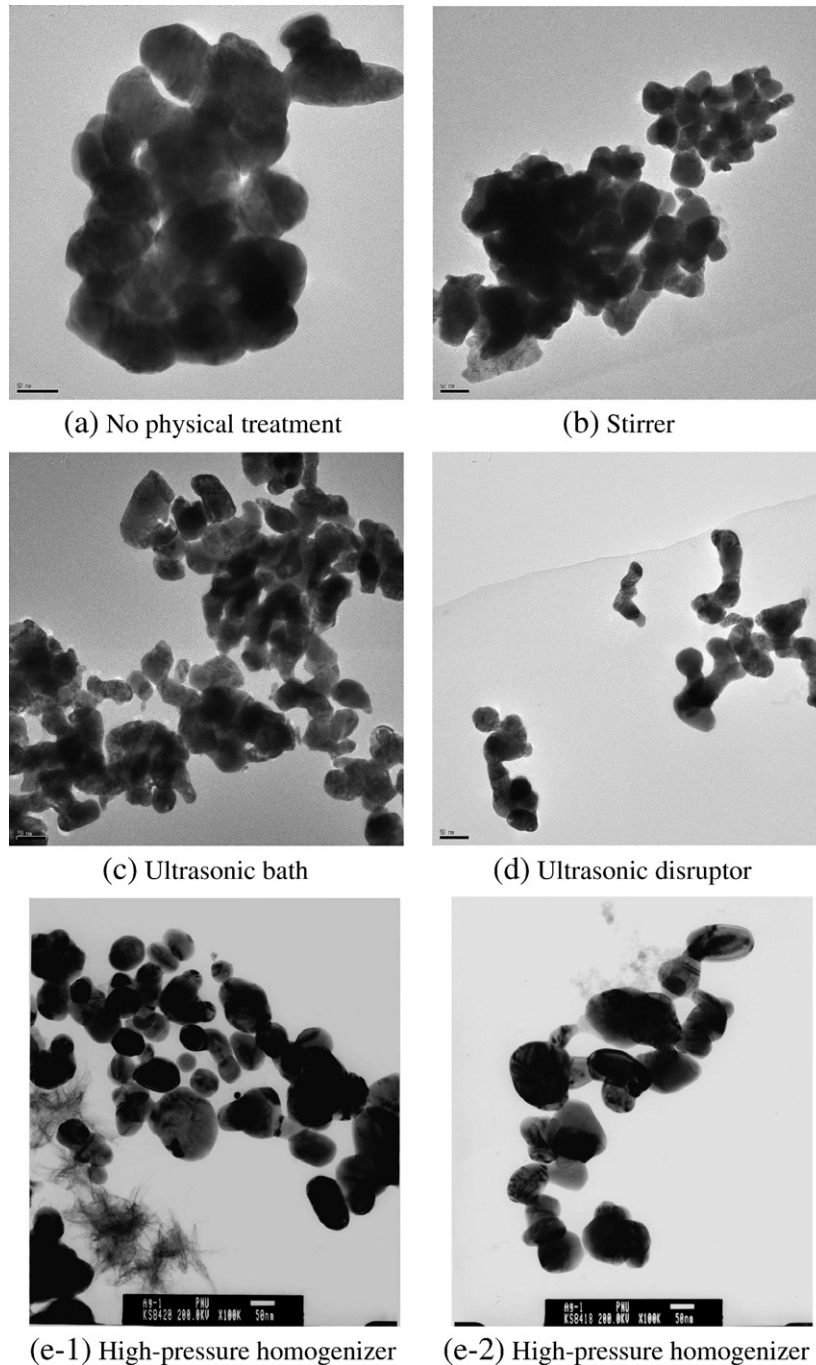
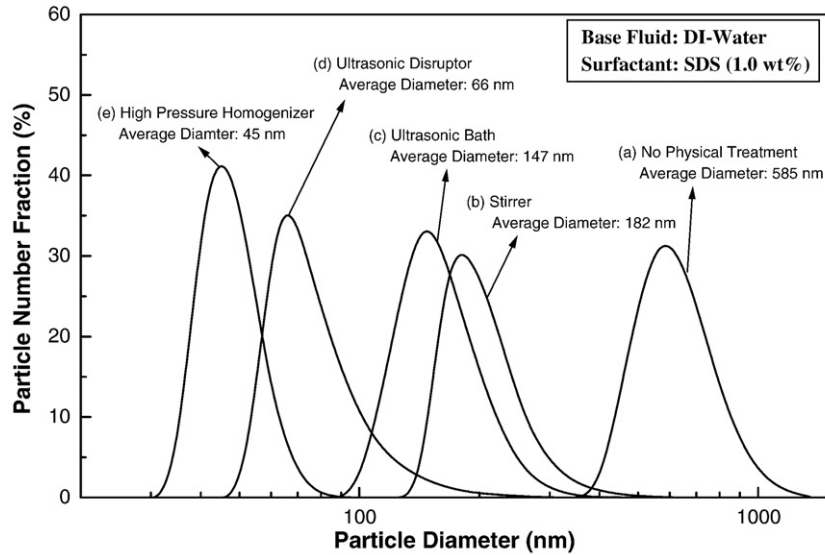


Fig. 5. TEM images of Ag particles in silicon oil-based nanofluids prepared by two-step methods. (The inserted scale bar is 50 nm).

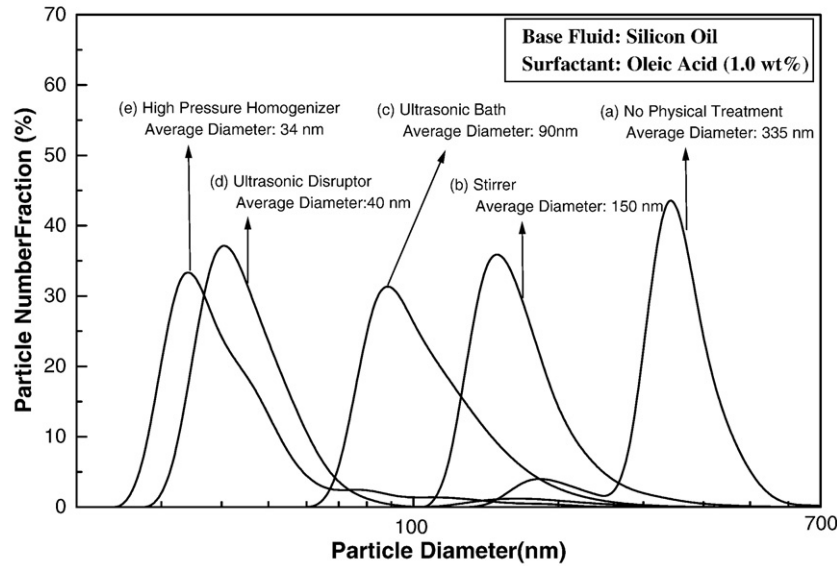
and Ag particles measured were 585 nm and 335 nm, respectively. After using various physical treatment techniques including the stirrer, the ultrasonic bath, the ultrasonic disruptor and the high-pressure homogenizer, the average diameter of CB nanoparticles was reduced to 182 nm, 147 nm, 66 nm, and 45 nm (see Fig. 6a), respectively, while for Ag nanoparticles, the average diameter of particles was reduced to 150 nm, 90 nm, 40 nm, and 35 nm (see Fig. 6b), respectively. These results indicate that the mechanical energy and cavitation energy generated by the stirrer and ultrasonication were not sufficient to break down the clusters of primary particles. However, the high-

pressure homogenizer was able to provide sufficient energy to deagglomerate the particle clusters with the combination of cavitations, shear force, and strong impaction on the nanoparticle clusters.

Now, we turn our attention to a one-step method for enhancing the dispersity of nanoparticles in the base fluid. To generate Ag nanoparticles, we employed the modified magnetron sputtering system, in which sputtered Ag nanoparticles were directly impacted on the silicon oil thin film formed on a rolling drum (see Fig. 3) for 20 min. Fig. 7a presents the TEM image of Ag nanoparticles produced by our modified magnetron



(a) CB-water nanofluids



(b) Ag-silicon nanofluids

Fig. 6. The particle size distributions in nanofluids as a function of the dispersion methods.

sputtering system. For the TEM analysis, Ag–silicon oil nanofluid was diluted with acetone with volume mixing ratio of nanofluid: acetone = 1:10. The Ag nanoparticles were relatively uniform with the primary size of less than 5 nm. This was also verified by particle size distribution measurement performed by ELS (see Fig. 7b), indicating that average diameter of Ag nanoparticle was ~3 nm and the particles were well-dispersed in the silicon oil because no agglomerated particles with larger particle diameter were observed. We believe that the formation of well-dispersed ~3 nm primary particles with less agglomeration was presumably resulted from the suppression of coagulation process between Ag primary particles in surfactant-presented base fluid. After producing Ag–silicon oil nanofluids with the assistance of the modified magnetron sputtering system, no sedimentation was

observed for ~60 days, indirectly indicating the long-term stability of the prepared Ag–silicon oil nanofluid.

To evaluate the dispersion stability of nanofluids prepared by various dispersion methods, we measured the zeta potential values of the CB nanoparticles dispersed in DI-water using ELS. The values of zeta potential ( $\zeta$ ) can be calculated by the Helmholtz–Smoluchowski equation [24],

$$\zeta = \mu U / \varepsilon \quad (1)$$

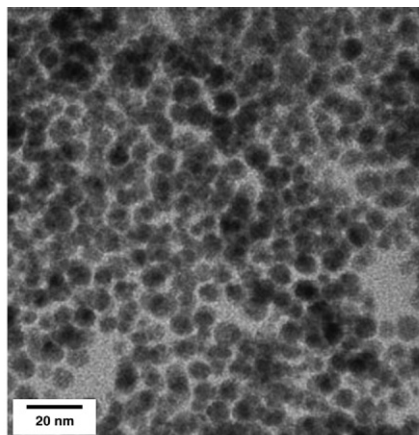
where  $U$  is the electrophoretic mobility, and  $\mu$  and  $\varepsilon$  are the viscosity and the dielectric constant of the liquid in the boundary layer, respectively.

The measured zeta potential of the CB nanoparticles suspended in water without surfactant prepared by the ultrasonic

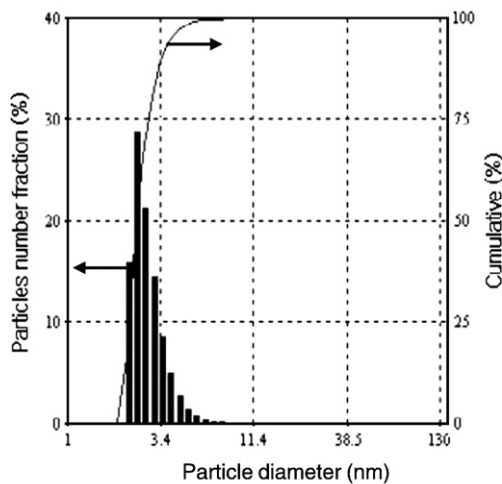


disruptor was found to be  $-1.27$  mV at pH 7.5. However, with the simple addition of the SDS (1 wt.%), the zeta potential of the CB nanoparticle fluid was significantly reduced to  $-26.25$  mV at the same pH level of 7.5. The zeta potentials of surfactant-added CB suspensions prepared with no physical treatment, stirrer, and high-pressure homogenizer were  $-20.84$ ,  $-25.11$  mV and  $-26.92$  mV, respectively. The zeta potential values of suspensions with surfactant treatment are almost similar. The small differences in zeta potentials measured for each type of physical treatment are in the range of measurement error. This indicates that the addition of SDS in CB nanofluids is presumably resulted in the strong electrostatic repulsion between the CB nanoparticles regardless of physical treatment, and it promotes the stabilization of the CB nanofluids.

Fig. 8 shows that the zeta potentials of the CB suspensions as a function of pH without and with SDS. These suspensions were prepared with the high-pressure homogenizer. Without SDS addition, the zeta potential of CB suspension was significantly decreased with increasing pH value. However, with the controlled-amount addition of SDS, the zeta potential of the CB



(a) TEM image



(b) Particle size distribution

Fig. 7. (a) TEM image and (b) the size distribution of Ag particles in silicon oil-based nanofluids prepared by the modified magnetron sputtering system (i.e. one-step method).

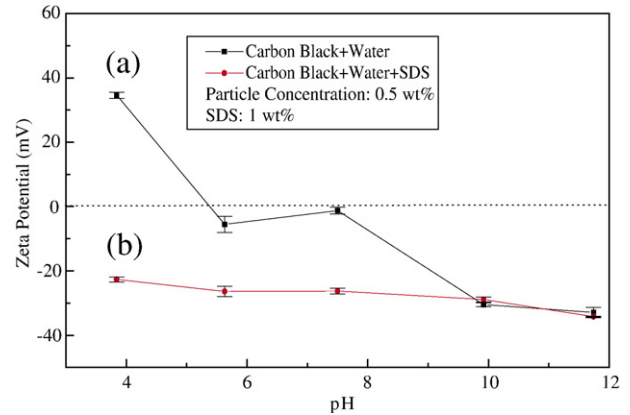


Fig. 8. The evolution of zeta potentials of the water-based CB nanofluids as a function of pH (a) without SDS and (b) with SDS (1 wt.%).

suspension remained at relatively low negative charge range regardless of pH value, indicating that the hydrophilic segment of the SDS added was presumably negatively ionized in the broad pH ranges [15].

After preparing various stable nanofluids, we previously measured the thermal conductivity of various nanofluids [27]. We observed that the relative thermal conductivity of nanofluid to pure fluid was reached up to  $\sim 5\%$  enhancement for CuO (1 Vol.%)–water nanofluid,  $\sim 9\%$  enhancement for CuO (1 Vol.%)–E.G. nanofluid, and  $\sim 3\%$  enhancement for fullerene (1.5 Vol.%)–mineral oil, which were kept constant due to the stability of the prepared nanofluids. To ensure the constant thermal properties of nanofluids, it is important to prepare nanofluids with the dispersion stability [28].

#### 4. Conclusions

In this work, we produced the CB–water and Ag–silicon oil nanofluids using two-step methods with the assistance of the stirrer, the ultrasonic bath, the ultrasonic disruptor and the high-pressure homogenizer, and also we produced Ag–silicon oil nanofluids using the one-step method with the assistance of the modified magnetron sputtering system.

Among the two-step methods, the most stable nanofluid was prepared by the high-pressure homogenizer. It is believed that the highly agglomerated nanoparticles were able to be easily broken by the combination of strong shear force and cavitation generated by the high-pressure homogenizer. We also observed that extremely stable nanofluid was able to be produced by the one-step method, in which we employed the modified magnetron sputtering system. The average diameter of Ag particles produced by the magnetron sputtering method was  $\sim 3$  nm, and no sedimentation was observed for 60 days. It is noted that the surfactants (i.e. SDS or oleic acid) plays key role to prepare stable nanofluids by increasing the magnitude of the zeta potential.

To get stable nanofluids, one should employ the high energy-assisted deagglomeration process of particle clusters dispersed in a base fluid with suitable surfactants. In this work, we have systematically tested the effect of various physical dispersing methods on dispersity and stability of nanoparticles in



nanofluids, which may provide useful guidelines for choosing a suitable method to prepare stable nanofluids in various nano-fluid-based applications.

### Acknowledgements

This work was financially supported by the Pusan National University Research Grant, the Ministry of Education and Human Resources Development (MOE), the Ministry of Commerce, the Industry and Energy (MOCIE), and the Ministry of Labor (MOLAB) through the fostering project of the Laboratory of Excellency.

### References

- [1] R.L. Webb, N.H. Kim, Principles of Enhanced Heat Transfer, 2nd editions, Taylor & Francis, New York, 2005 Chapter 17, and references therein.
- [2] J.H. Ku, H.H. Cho, J.H. Koo, S.G. Yoon, J.K. Lee, (2000), Heat transfer characteristics of liquid–solid suspension flow in a horizontal pipe, *KSMIE International Journal* 14 (2000) 1159–1167.
- [3] Y. Xuan, Q. Li, Investigation on convective heat transfer and flow features of nanofluids, *Journal of Heat Transfer—Transaction of ASME* 125 (2003) 151–156.
- [4] Hrishikesh E. Patel, Sarit K. Das, T. Sundararajan, A. Sreekumaran Nair, Beena George, T. Pradeep, Thermal conductivities of naked and monolayer protected metal nanoparticle based nanofluids: manifestation of anomalous enhancement and chemical effects, *Applied Physics Letter* 83 (2003) 2931–2933.
- [5] B.M. Ginzburg, L.A. Shibaev, O.F. Kireenko, A.A. Shepelevskii, M.V. Baidakova, A.A. Sitnikova, Antiwear effect of Fullerene C60 additives to lubricating oils, *Russian Journal of Applied Chemistry* 75 (2002) 1330–1335.
- [6] Z. Libin, L. Xiulun, A study on boiling heat transfer in three-phase circulating fluidized bed, *Chemical Engineering Journal* 78 (2000) 217–223.
- [7] B. Yang, Z.H. Han, Thermal conductivity enhancement in water-in-FC72 nanoemulsion fluids, *Applied Physics Letters* 88 (2006) 261914.
- [8] Z.H. Han, B. Yang, S.H. Kim, M.R. Zachariah, Application of hybrid sphere/carbon nanotube particles in nanofluids, *Nanotechnology* 18 (2007) 105701.
- [9] C.H. Li, G.P. Peterson, Experimental investigation of temperature and volume fraction variations on the effective thermal conductivity of nanoparticle suspensions (nanofluids), *Journal of Applied Physics* 99 (2006) 084314.
- [10] Y. Hwang, H.S. Park, J.K. Lee, W.H. Jung, Thermal conductivity and lubrication characteristics of nanofluids, *Current Applied Physics* 6S1 (2006) e67–e71.
- [11] P. Keblinski, S.R. Phillpot, S.U.S. Choi, J.A. Eastman, Mechanisms of heat flow in suspensions of nano-sized particles (nanofluids), *International Journal of Heat and Mass Transfer* 45 (2002) 855–863.
- [12] D. Wasan, A. Nikolov, B. Moudgil, Colloidal dispersions: structure, stability and geometric confinement, *Powder Technology* 153 (2005) 135–141.
- [13] H. Yoshida, T. Nurtono, K. Fukui, A new method for the control of dilute suspension sedimentation by horizontal movement, *Powder Technology* 150 (2005) 9–19.
- [14] Y. Ding, D. Wen, Particle migration in a flow of nanoparticle suspensions, *Powder Technology* 149 (2005) 84–92.
- [15] L. Jiang, L. Gao, J. Sun, Production of aqueous colloidal dispersions of carbon nanotubes, *Journal of Colloid and Interface Science* 260 (2003) 89–94.
- [16] H. Xie, H. Lee, W. Youn, M. Choi, Nanofluids containing multiwalled carbon nanotubes and their enhanced thermal conductivities, *Journal of Applied Physics* 94 (2003) 4967–4971.
- [17] J.H. Fendler, Colloid chemical approach to nanotechnology, *Korean Journal of Chemical Engineering* 18 (2001) 1–6.
- [18] S.U.S. Choi, Z.G. Zhang, W. Yu, F.E. Lockwood, E.A. Grulke, Anomalous thermal conductivity enhancement in nanotube suspensions, *Applied Physics Letter* 79 (2001) 2252–2254.
- [19] K. Kameyama, T. Takagi, Micellar properties of octylglucoside in aqueous solutions, *Journal of Colloid and Interface Science* 137 (1990) 1–10.
- [20] T. Imae, N. Hayashi, Electrophoretic light scattering of alkyl- and oleyldimethylamine oxide micelles, *Langmuir*, 9 (1993) 3385–3388.
- [21] W.C. Hinds, *Aerosol Technology: Properties, Behavior, and Measurement of Airborne Particles*, John Wiley & Sons, 1982 Chapter 3.
- [22] P. Paquin, Technological properties of high pressure homogenizers: the effect of fat globules, milk proteins, and polysaccharides, *International Dairy Journal* 9 (1999) 329–335.
- [23] D.J. Shaw, *Introduction to colloid and surface chemistry*, Butterworth press, London, 1980.
- [24] B.R. Munson, D.F. Young, T.H. Okiishi, *Fundamentals of Fluid Mechanics*, 3rd editions, John Wiley & Sons, 1998 Chapter 3.
- [25] M. Wagener, B. Günther, Sputtering on liquids — a versatile process for the production of magnetic suspensions, *Journal of Magnetism and Magnetic Materials* 202 (1999) 41–44.
- [26] I. Nakatani, T. Furubayashi, T. Takahashi, H. Hanaoka, Preparation and magnetic properties of colloidal ferromagnetic metals, *Journal of Magnetism and Magnetic Materials* 65 (1987) 261–264.
- [27] Y. Hwang, J.K. Lee, C.H. Lee, Y.M. Jung, S.I. Cheong, C.G. Lee, B.C. Ku, S.P. Jang, Stability and thermal conductivity characteristics of nanofluids, *Thermochimica Acta*, 455 (2007) 70–74.
- [28] K.S. Hong, T. Hong, H. Yang, Thermal conductivity of Fe nanofluids depending on the cluster size of nanoparticles, *Applied Physics Letters* 88 (2006) 031901.